JOURNAL OF TISSUE ENGINEERING AND REGENERATIVE MEDICINE
J Tissue Eng Regen Med 2016.
Published online in Wiley Online Library (wileyonlinelibrary.com) **DOI:** 10.1002/term.2170

RESEARCH ARTICLE

Differentiation of adipose stem cells seeded towards annulus fibrosus cells on a designed poly(trimethylene carbonate) scaffold prepared by stereolithography

Sébastien B.G. Blanquer[1,2†], Arjen W.H. Gebraad[1,3†], Susanna Miettinen[4], André A. Poot[1,2], Dirk W. Grijpma[1,2,5] and Suvi P. Haimi[1,3*]

[1]*MIRA Institute for Biomedical Technology and Technical Medicine, Department of Biomaterials Science and Technology, University of Twente, Enschede, the Netherlands*
[2]*Collaborative Research Partner Annulus Fibrosus Rupture Program of AO Foundation, Davos, Switzerland*
[3]*Department of Oral and Maxillofacial Sciences, Clinicum, University of Helsinki, Helsinki, Finland*
[4]*Institute of Biosciences and Medical Technology (BioMediTech), University of Tampere, Tampere, Finland*
[5]*University of Groningen, University Medical Centre Groningen, W.J. Kolff Institute, Department of Biomedical Engineering, Groningen, the Netherlands*

'Correction added on 14 November 2016, after first online publication: The Author requested to update the order of affiliations.'

Abstract

Cell-based therapies could potentially restore the biomechanical function and enhance the self-repair capacity of annulus fibrosus (AF) tissue. However, choosing a suitable cell source and scaffold design are still key challenges. In this study, we assessed the *in vitro* ability of human adipose stem cells (hASCs), an easily available cell source to produce AF-like matrix in novel AF-mimetic designed scaffolds based on poly(trimethylene carbonate) and built by stereolithography. To facilitate efficient differentiation of hASCs towards AF tissue, we tested different culture medium compositions and cell seeding techniques. This is the first study to report that medium supplementation with transforming growth factor (TGF)-β3 is essential to support AF differentiation of hASCs while TGF-β1 has negligible effect after 21 days of culture. Fibrin gel seeding resulted in superior cell distribution, proliferation and AF-like matrix production of hASCs compared to direct and micromass seeding under TGF-β3 stimulation. Not only the production of sulphated glycosaminoglycans (sGAG) and collagen was significantly upregulated, but the formed collagen was also oriented and aligned into bundles within the designed pore channels. The differentiated hASCs seeded with fibrin gel were also found to have a comparable sGAG:collagen ratio and gene expression profile as native AF cells demonstrating the high potential of this strategy in AF repair. Copyright © 2016 John Wiley & Sons, Ltd.

Received 17 June 2015; Revised 6 January 2016; Accepted 10 February 2016

Keywords **AF-mimetic designed scaffold; poly(trimethylene carbonate) PTMC; stereolithography; human adipose stem cells (hASCs); oriented collagen fibres; annulus fibrosus; tissue engineering**

1. Introduction

The annulus fibrosus (AF) is a multilamellar fibrocartilaginous tissue that forms the outer layer of the intervertebral disc (IVD) and is subjected to high risk of degeneration because of its avascularity and low cellularity (Bibby *et al.*, 2001). Degeneration of the IVD leads to tearing of the AF (Coppes *et al.*, 1990). Even minor injuries to the AF can lead to permanent disc damage (Fazzalari *et al.*, 2001). The conventional treatments by drug administration (Blanquer *et al.*, 2015) and/or established surgical methods have shown serious drawbacks and limited success (Bao *et al.*, 1996; Disch *et al.*, 2008). Therefore, new effective treatments are urgently needed. Tissue engineering of AF is a promising approach allowing immediate closure of the defect, restoring the biomechanical properties of the disc and simultaneously encouraging the repair of the ruptured tissue.

Several scaffold processing techniques with different types of biodegradable biomaterials have been suggested for AF tissue engineering (Guterl *et al.*, 2013). Unfortunately, none of the current strategies have been able to attain the biomechanical properties of the native AF tissue and restore its function. A major challenge has been the reproduction of the complex multilamellar structure and the biomechanical cues of the native tissue (Figure 1a,b) (Ebara *et al.*, 1996; Nerurkar *et al.*, 2010), which are prerequisites for efficient cell differentiation and extracellular matrix (ECM) organization (Guterl *et al.*, 2013). Therefore, a scaffold for AF regeneration must preferably induce the specific orientation and direction of the collagen bundles. An accurately-controlled three-dimensional (3D) scaffold preparation method that is able to reproduce the complex organization and orientation of the pore characteristics of the damaged tissue has not yet been reported. Stereolithography could be used to create these complex designs as it is known to be a most versatile 3D structure processing method, with the highest accuracy and precision (Melchels *et al.*, 2010; Skoog *et al.*, 2014) of additive manufacturing techniques.

*Correspondence to: S. P. Haimi, Department of Oral and Maxillofacial Sciences, Clinicum, Faculty of Medicine, PO Box 41, University of Helsinki, 00014Helsinki, Finland. E-mail: suvi.haimi@helsinki.fi
†These authors contributed equally to this work.

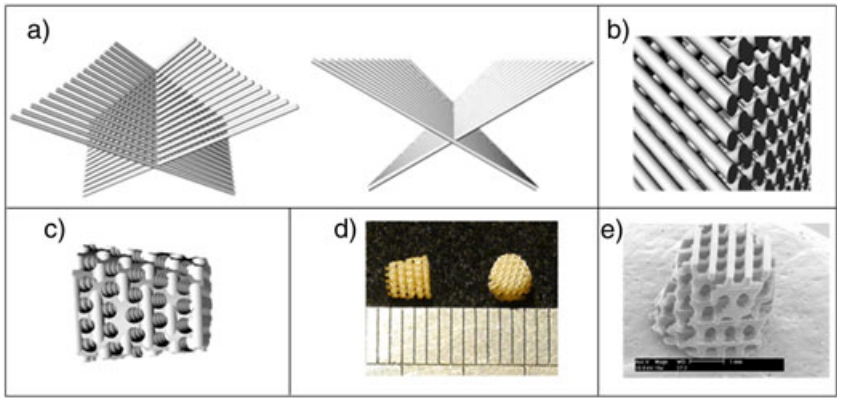

Figure 1. Schematic illustration of alternating collagen fibre architecture (a) showing the typical overlapping organization and angle-ply fibres (from 30° to 45°) of the native annulus fibrosus (AF). (b) Schematic illustration of organized collagen bundle layers in the native AF. (c) Computer-aided design representation of the three-dimensional scaffold with the pore channels that follow the orientation from peripheral to central as the collagen fibres in the native AF tissue. (d) Photographic image of the poly(trimethylene carbonate) (PTMC) scaffolds built by stereolithography. (e) High resolution SEM image of the PTMC scaffold built.

In addition to the scaffold design and preparation challenge, a suitable cell source and efficient differentiation method need to be available for successful cell therapy leading to functional AF matrix synthesis and disc regeneration. Although autologous AF cell transplantation therapies have had some success in animal models (Kuh *et al.*, 2009), an alternative for clinical therapy is ineluctably required because of the limited availability and expansion capacity of autologous AF cells (Bron *et al.*, 2009). Bone marrow-derived mesenchymal stem cells (BMSCs) have been used for AF tissue engineering applications (Richardson *et al.*, 2010; Orozco *et al.*, 2011). However, the use of these cells is also limited by the quantity that can be collected from the patient, and by the associated donor-site morbidity. The use of multipotent human adipose stem cells (hASCs) differentiated towards an AF phenotype could avoid these problems as adipose tissue is an abundant and easily accessible cell source (Lindroos *et al.*, 2011). Interestingly, recent studies have shown that isoforms of transforming growth factor-β (TGF-β) can stimulate the differentiation of animal- and human-derived ASCs towards an AF phenotype (Tapp *et al.*, 2008; Gruber *et al.*, 2010). However, a systematic comparison between the key isoforms of TGF-β, type 1 and type 3, and their use in combination to efficiently differentiate hASCs towards an AF phenotype is lacking.

In this study we aimed to establish an effective method to engineer AF tissue using novel AF-mimetic designed scaffolds seeded with hASCs and differentiated *in vitro* under optimized culture conditions. This is the first study describing the preparation of a tissue engineering scaffold with a pore architecture representing the orientation of the collagen bundles of the AF tissue. Because both mechanical properties and the architecture of the scaffold play an important role in the biological response, we propose to use resins based on poly(trimethylene carbonate) (PTMC). This polymer is known for its biocompatibility and biodegradability (Zhang *et al.*, 2006; Vyner *et al.*, 2014) but also for its rubber-like properties (Schuller-Ravoo *et al.*, 2013). To allow effective hASC differentiation towards AF tissue, a new hASC differentiation strategy was established, based on optimization of seeding method and TGF-β1 and TGF-β-3 isoform supplementation.

2. Materials and methods

2.1. Scaffold fabrication and characterization

The scaffolds were designed using 3D software Rhinoceros 3D (McNeel Europe, Barcelona, Spain) and K3dSurf v. 0.6.2, GNU-General public legend (http://k3dsurf.sourceforge.net).

The synthesis of PTMC oligomers (M_n = 5000 g/mol) was carried out by ring-opening polymerization of 0.98 mol (100 g) trimethylene carbonate (1,3-dioxan-2-one; TMC, Foryou Medical, Huizhou City, China), initiated by 0.0196 mol (2.62 g) tri(hydroxymethyl)propane (TMP; Sigma-Aldrich, Munich, Germany) and catalysed by 0.05 wt% stannous octoate (tin 2-ethylhexanoate, SnOct2; Sigma-Aldrich) at a temperature around 130°C for 3 days under an argon atmosphere. Subsequently, the oligomer was end-functionalized with methacrylate groups using 0.18 mol (27 ml) of methacrylic anhydride in the presence of 0.18 mol (25 ml) of triethylamine in solution in dichloromethane (100 ml) (Sigma-Aldrich) at room temperature under an argon atmosphere for 5 days.

Proton nuclear magnetic resonance (1H-NMR, 300 MHz) was used to determine the conversion rate and the number average molecular weight (M_n) of the macromer. The resin for stereolithography was prepared by dilution of the PTMC macromer in propylene carbonate (Sigma-Aldrich) to reach a viscosity of approximately 5–10 Pa.s. The resin further contained Lucirin TPO-L (5 wt % relative to the macromer) (BASF, Ludwigshafen am Rhein, Germany) as a photo-initiator and Orasol Orange dye (0.15 wt% relative to the macromer) (Ciba Speciality Chemicals, Basel, Switzerland) to control the penetration depth of the UV light. The scaffolds were built using a UV stereolithograph (EnvisionTech Perfactory, Gladbeck, Germany) at a pixel resolution 16 × 16 μm^2 and a layer thickness of 100 μm per layer. To reach this resolution with this resin composition, the illumination time per layer was 20 s with a light intensity of 180 mW/cm^2. After extraction twice for 6 h in acetone (Sigma-Aldrich), the scaffolds were washed with 70% ethanol (Sigma-Aldrich) for six more hours and dried until a constant weight was reached.

DOI: 10.1002/term

The mechanical properties of the scaffolds were measured by compression testing in the dry state using a material testing machine (Zwick Z020; Ulm, Germany), equipped with a 500 N load cell at a compression rate of 30% per minute to a maximum of 80% strain.

Scanning electron microscopy (SEM) (Philips XL30 ESEM-FEG; Philips, Amsterdam, the Netherlands) was applied to visualize the porous structures. The specimens were sputter-coated with gold and the apparatus was operated at a voltage of 3 kV.

2.2. Adipose stem cell isolation and characterization

Human ASCs were isolated from six female donors (age 52 ± 9 years) and expanded in maintenance medium (MM; Table 1) at 37°C and 5% carbon dioxide (CO_2) as previously described (Kyllonen *et al.*, 2013). The study was carried out under approval of the ethical committee of Pirkanmaa Hospital District and with informed consent from the donors.

After expansion, hASCs were characterized by flow cytometry (BD Biosciences, San Jose, CA USA) to confirm the mesenchymal origin of the cells. Monoclonal antibodies against CD14-PE-Cy7, CD19-PE-Cy7, CD45RO-APC, CD73-PE and CD90-APC (BD Biosciences), HLA-DR-PE (ImmunoTools GmbH, Friesoythe, Germany) and CD11a-APC, CD80-PE, CD86-PE, and CD105-PE (R&D Systems Inc., Minneapolis, USA) were used. Analysis was performed on 10 000 cells per sample and positive expression was defined as the level of fluorescence greater than 99% of the corresponding unstained cell sample.

2.3. Differentiation medium component optimization in micromass cultures

To optimize the AF differentiation medium for hASCs, a preliminary screening of the potential growth factors was done in a micromass culture. For this, hASCs at passages three to four were plated according to the micromass culture technique described earlier (Tapp *et al.*, 2008) in order to stimulate AF differentiation. A high cell density suspension (10^7 cells/ml) was added as three droplets of 10 μl to the centre of wells in 24-well plates (Nunc, ThermoFisher Scientific, Waltham, MA USA). Cultures were incubated for 3 h before the addition of 700 μl control CM, or differentiation media consisting of CM supplemented with either 10 ng/ml TGF-β1 (DM1), 10 ng/ml TGF-β3 (DM3) or 10 ng/ml each of TGF-β1 and TGF-β3 (DM1 + 3) (Table 1). A concentration of 10 ng/ml was used as this concentration for both TGF-β1 and TGF-β3 has been shown previously to be effective for hASCs (Gruber *et al.*, 2010). Experiments were repeated three times with different donors. Technical duplicates of each sample were used in all assays. After 14 days and 21 days of culture, the micromasses were collected for biochemical, histological and polymerase chain reaction (PCR) analysis. The DM3 medium was selected as the AF differentiation medium for the subsequent scaffold experiments based on the obtained results (see section 2.1).

Table 1. The compositions of mediums used in the study

Medium	Composition
Maintenance medium (MM)	DMEM-F12 (Gibco, ThermoFisher Scientific, Waltham, MA USA); 5–10% human serum (PAA Laboratories GmbH, Pasching, Austria); 1% antibiotics (100 U/ml penicillin; 100 μg/ml streptomycin; Lonza Biowhittaker, Verviers, Belgium); 1% vol L-alanyl-L-glutamine (Glutamax I, Gibco)
Control chondrogenic medium (CM)	DMEM-F12 (Gibco); ITS + 1 (BD Biosciences San Jose, CA USA); 0.3% vol antibiotics (100 U/ml penicillin; 100 μg/ml streptomycin; Lonza); 1% vol L-alanyl-L-glutamine (Glutamax I; Gibco); 50 μg/ml L-ascorbic acid 2-phosphate (Sigma-Aldrich, Munich, Germany); 55 μg/ml sodium pyruvate (Lonza); 23 μg/ml L-proline (Sigma-Aldrich)
DM1	CM containing 10 ng/ml TGF-β1 (Santa Cruz, Dallas, TX, USA)
DM3	CM containing 10 ng/ml TGF-β3 (Prospec, Rehovot, Israel)
DM1 + 3	CM containing 10 ng/ml TGF-β1, 10 ng/ml TGF-β3

TGF, transforming growth factor.

2.4. Adipose stem cell seeding in scaffolds

The scaffolds were pre-treated with CM 24 h before cell seeding. At passages 3–4, hASCs were seeded in the scaffolds using micromass, fibrin or direct seeding. In the micromass seeding group, hASCs were suspended in MM at high cell density (10^7 cells/ml) as described in section 1.3, and two cell suspension droplets of 10 μl were carefully applied to the lateral sides of the scaffold. In the fibrin seeding group, 180 000 hASCs were suspended in 20 μl of fibrinogen solution (33.3 mg/ml) and then combined with 20 μl of thrombin solution (1 U/ml) immediately before pipetting into the scaffold (Baxter Biosurgery, Vienna, Austria). In the direct seeding group, 180 000 hASCs were suspended in 40 μl of MM and pipetted directly into the scaffold. It should be noted that in the direct and fibrin seeding, the initial cell number was 10% lower compared with micromass seeding. The maximum number of cells that could be kept in suspension in a 40 μl volume was 180 000. A single cell suspension is critical for direct seeding. The cell-seeded scaffolds were incubated at 37°C and 5% CO_2 for 3 h (micromass and direct seeding groups) to allow cell attachment or for 1 h (fibrin seeding group) to allow fibrin gelation before transferring the scaffolds to new wells in 24-well plates (Nunc) with 1 ml of DM3. Scaffolds with pure fibrin gel without hASCs were used as blanks in all the assays to take into account the background caused by the fibrin gel in the assays. In the direct- and micromass-seeding groups, scaffolds without fibrin and without hASCs were used as blanks. Experiments were repeated three times with different donors. Technical duplicates of each sample were used in all assays. After 1, 14 and 21 days of culture, the cell-seeded scaffolds were collected for biochemical, histological and PCR analysis.

2.5. Annulus fibrosus cell culture in scaffolds

Human AF cells (ScienCell Research Laboratories, Carlsbad, CA, USA) seeded with fibrin gel (human AF cells; ScienCell) were used as a reference cell type in order to verify the

DOI: 10.1002/term

phenotype of the differentiated hASCs towards AF tissue. Fibrin gel-seeded AF cells have previously been shown to maintain the typical features of these cell populations (Colombini *et al.*, 2014). Human AF cells were expanded according to the manufacturer's protocol in a commercially available medium (NPCM; ScienCell) at 37°C, 5% CO_2. After expansion, cells from passage 4 were seeded into the scaffolds using fibrin gel seeding, as described in detail in section 1.4. After 2 weeks and 3 weeks of culture, scaffolds were collected for biochemical and PCR analysis.

2.6. Biochemical analysis of the micromass cultures and the cell-seeded scaffolds

For biochemical analysis, micromass cultures were digested for 48 h with 1.25 U/ml papain (Sigma-Aldrich) at pH 6.5 and 65°C. Cell-seeded scaffolds were rinsed with PBS and digested overnight under identical conditions. The amount of DNA in the micromass culture lysates was quantified using 0.2 μg/ml Hoechst 33258 nucleic acid stain (Bio-Rad Laboratories Inc., Hercules, CA, USA) with purified calf thymus DNA as a standard (Bio-Rad). Fluorescence was measured with a multiplate reader (Victor 1420 Multilabel Counter; Wallac, Turku, Finland) using excitation at 360 nm and emission at 460 nm. The amount of DNA in the cell-seeded scaffold lysates was evaluated by using the CyQuant proliferation assay (Invitrogen, Carlsbad, CA, USA) as previously described by our group (Haimi *et al.*, 2009a). A standard curve was prepared by serial dilution of bacteriophage λDNA (Invitrogen). Fluorescence (excitation at 480 nm, emission at 520 nm) was measured using a microplate reader (Infinite 200 PRO series; Tecan, Männedorf, Switzerland).

The total amount of sulphated glycosaminoglycans (sGAG) in the papain lysates of the micromass cultures and the cell-seeded scaffolds was analysed with a sGAG assay kit (Blyscan; Biocolor Ltd, Carrickfergus, UK) according to manufacturer's instructions. A standard from the kit consisting of chondroitin 4-sulphate sodium salt from bovine trachea was used in order to quantify the total amount of sGAG. Absorbance was measured at 656 nm in a multiplate reader (Victor, PerkinElmer, Waltham, MA USA).

The total collagen content of the cell-seeded scaffolds was quantified using a hydroxyproline assay (Sigma-Aldrich). The papain lysate was hydrolysed in 6 N hydrochloric acid solution (Sigma-Aldrich) at 110°C for 3 h followed by quantification of hydroxyproline content based on the reaction of oxidized hydroxyproline with 4-(dimethylamino)benzaldehyde (DMAB). Absorbance was measured at 544 nm in the multiplate reader (Victor). Collagen content was calculated based on the reported weight ratio of hydroxyproline to collagen of 0.125 (Edwards and Obrien, 1980), assuming that elastin content was negligible.

2.7. Histological staining

Micromass cultures were fixed for 1 h in 4% paraformaldehyde (Sigma-Aldrich), embedded in paraffin and sectioned at 5 μm thickness for histological analysis. Proteoglycan production in the extracellular matrix (ECM) was assessed by toluidine blue staining (0.1% volume in distilled water; Sigma-Aldrich) (Tapp *et al.*, 2008).

Cell attachment and distribution in the scaffolds was evaluated using methylene blue staining. Before methylene blue (Sigma-Aldrich) staining, the scaffolds were fixed in 4% paraformaldehyde solution. After fixation, cells were stained with methylene blue solution [1% in borax; B-3545 Borax (99.5–105%), Sigma Aldrich] and rinsed with phosphate-buffered saline (PBS) to eliminate the excess of methylene blue. Subsequently, cell attachment and distribution in the scaffold was assessed using a stereomicroscope [Nikon SMZ-10 A (Nikon, Tokyo, Japan) with Sony 3CCD camera (Sony, Tokyo, Japan)].

To evaluate collagen deposition, the cell-seeded scaffolds were fixed in 4% paraformaldehyde solution, transferred to 5% sucrose (Sigma-Aldrich) overnight, embedded in Jung tissue freezing medium (Leica, Wetler, Germany) and frozen at −20°C. Subsequently, the scaffolds were sectioned at 14 μm thickness using a Shandon cryotome (Cryostat series; Shandon, Eragny sur oise, France). The cross-sections were placed on glass slide and then dried for 3 days. The production of collagen in the cell-seeded scaffolds was evaluated by PicroSirius Red (Polysciences, Inc., Warrington, PA USA) staining following the supplier's protocol. The microscopic preparations were visualized with a Nikon E600 Fluorescence/Histology microscope. Polarized light was used to detect oriented collagen fibres.

2.8. Gene expression of differentiated hASCs and native AF cells

Quantitative reverse transcription polymerase chain reaction (qRT-PCR) was used to study the relative expression of AF phenotype-related genes in micromass cultures and in cell-seeded scaffolds. Total RNA was isolated using the NucleoSpin® RNA II Total RNA isolation kit (Macherey-Nagel GmbH & Co., KG, Düren, Germany) according to the manufacturer's instructions. Total RNA yield was measured by optical density at 260 nm with a Nanodrop 1000 spectrophotometer (Thermo Fisher Scientific, Waltham, MA, USA), and sample purity was assessed from the ratio of A260/A280. The iScript cDNA Synthesis Kit (Bio-Rad, Hercules, CA, USA) was used to prepare cDNA from the total RNA. Reverse transcription was performed using a Bio-Rad CFX96 Real-Time PCR system.

Gene expressions of aggrecan, decorin, and collagen type I type II were analysed in micromass cultures. Moreover, collagen type V expression was also analysed in the cell-seeded scaffolds. Gene expression was assessed by PCR analysis using human acidic ribosomal phosphoprotein P0 (RPLP0) as a reference gene, which has been shown to be stably expressed under several experimental conditions (Gabrielsson *et al.*, 2005; Fink *et al.*, 2008). The primer sequences (Sigma-Aldrich) are presented in Table 2.

DOI: 10.1002/term

Table 2. Reverse and forward primer sequences used for polymerase chain reaction assay

Gene		Primer sequence	Product size (bp)
Acidic ribosomal phosphoprotein P0	Forward	5′-AAT CTC CAG GGG CAC CAT T-3′	70
	Reverse	5′-CGC TGG CTC CCA CTT TGT-3′	
Aggrecan	Forward	5′-TCG AGG ACA GCG AGG CC-3′	85
	Reverse	5′-TCG AGG GTG TAG CGT GTA GAG A-3′	
Decorin	Forward	5′-CTC TGC TGT TGA CAA TGG CTC TCT-3′	135
	Reverse	5′-TGG ATG GCT GTA TCT CCC AGT ACT-3′	
Collagen type I	Forward	5′-CCA GAA GAA CTG GTA CAT CAG CAA-3′	140
	Reverse	5′-CGC CAT ACT CGA ACT GGA ATC-3′	
Collagen type II	Forward	5′-GAG ACA GCA TGA CGC CGA G-3′	67
	Reverse	5′-GCG GAT GCT CTC AAT CTG GT-3′	
Collagen type V	Forward	5′-TGA GTT GTG GAG CTG ACT CTA ATC-3′	181
	Reverse	5′-TAA CAG AAG CAT AGC ACC TTT CAG-3′	

Reaction mixtures contained a maximum of 50 ng cDNA, 300 nM forward and reverse primers and Power SYBR® Green PCR Master Mix (Applied Biosystems, Foster City, CA, USA). The PCR reactions were conducted in duplicates and monitored using the ABI Prism® 7300 Sequence Detection System (Applied Biosystems) starting with initial activation at 95°C for 10 min, followed by 45 cycles of denaturation at 95°C for 15 s and annealing and extending at 60°C for 60 s. The results were normalized to expression of RPLP0 according to a mathematical model described by Pfaffl (2001).

2.9. Statistical analysis

Statistical analyses were performed with SPSS version 20 (IBM, Armonk, NY, USA). The effects of medium composition, cell seeding technique and culture duration on DNA content, sulphated GAG content, collagen content and normalized gene expression levels were analysed using Kruskal–Wallis one-way analysis of variance by ranks, followed by a Mann–Whitney *U post hoc* test to analyse specific sample pairs for significant differences. The results were considered significant when $p < 0.05$.

3. Results

3.1. Structural and mechanical scaffold characterization

A truncated cone design was built with a height of 4 mm, a maximum diameter of 4 mm and a minimum diameter of 3 mm. The scaffolds built had a porosity of 76% with an average pore channel diameter of 420 μm (Figure 1c). In order to reproduce the function and the structure of the AF tissue, the pore channels mimic the organization and the orientation of collagen fibres from native AF tissue.

The compression modulus of the cubic porous PTMC scaffolds designed was 0.35 ± 0.10 MPa. This indicates that the scaffolds are flexible, possibly allowing shearing between different lamellae of the native AF (Nerurkar *et al.*, 2009). In future work, the mechanical properties of the scaffolds during the whole culture period should be evaluated.

3.2. Adipose stem cell characterization

Human ASCs demonstrated high expression (>85%) of CD90 (Thy-1) and CD105 (endoglin), moderate (>50%) or high expression of CD73 (ecto 5′ nucleotidase) and no or low expression (≤2%) of CD11a (lymphocyte function-associated antigen 1), CD14 (monocyte and macrophage marker), CD19 (dendritic cell marker), CD45RO (pan-leukocyte marker), CD80 (B-cell marker), CD86 (antigen presenting cell marker), and HLA-DR [human leukocyte antigen (HLA) class II]. The results showed that hASCs expressed most of the specific antigens that define human stem cells of mesenchymal origin according to the Mesenchymal and Tissue Stem Cell Committee of the ISCT (Dominici *et al.*, 2006).

3.3. Optimization of differentiation medium components in micromass cultures

The biochemical analyses of the micromasses revealed that the numbers of hASCs were significantly higher at both the 14- and 21-day time-points in the presence of TGF-β3 (DM3 and DM1 + 3) compared with the CM group (see the Supplementary material online, Figure 1a). The total cell number did not increase with time in any of the groups. The addition of TGF-β3 resulted in significantly higher amounts of sGAGs in the DM3 and DM1 + 3 groups compared with the CM group at 21 days of culture (see the Supplementary material online, Figure S1b).

These results were consistent with toluidine blue staining (see the Supplementary material online, Figure S1c). Samples cultured in the presence of TGF-β3 had more specific staining of the proteoglycans compared with samples cultured in CM or DM1 at both time-points. The highest proteoglycan content was found in samples cultured in DM3 for 14 days. At the 21-day time-point, micromasses cultured in CM were notably smaller compared with samples cultured in the presence of TGF-β1 and/or TGF-β3.

The analysis of AF-specific genes in the micromass cultures at 21 days showed the highest aggrecan expressions in hASCs cultured in the presence of TGF-β3 (see the Supplementary material online, Figure S1d). However, owing to donor variation, no significant differences were found. Consistent with the biochemical analysis and the toluidine blue staining, the addition of TGF-β1 alone (DM1) or in combination with TGF-β3 (DM1 + 3) did not significantly increase the aggrecan expression compared with the groups without TGF-β1 (CM and DM3, respectively). The expressions of decorin, collagen type I and type II between the medium groups were not different (data not shown). Based on these results, DM3 was selected for further experiments.

3.4. Methylene blue staining of the seeded scaffolds

Major differences between the different seeding methods were observed at day 1 as only fibrin gel seeding allowed

DOI: 10.1002/term

homogeneous methylene blue staining, indicating uniform hASC distribution in the scaffolds (Figure 2). The fibrin gel alone did not significantly take up the methylene blue dye, as demonstrated in the Supplementary material online (Figure S2). With micromass- and direct-seeding of the cells only few areas were stained by the methylene blue, suggesting poor cell attachment in the scaffolds. At day 14, the differences were even more pronounced as only with fibrin gel seeding were hASCs homogeneously attached throughout the scaffold. Instead, hASCs seeded by micromass seeding grew in clusters only near the original seeding sites. Direct seeding led to poor distribution of hASCs during the 14-day culture period.

3.5. Biochemical analysis of the seeded scaffolds

Consistent with the results of methylene blue staining, direct seeding in the scaffolds showed significantly lower cell seeding efficiency and proliferation of hASCs compared with the other seeding methods at all measured time-points (Figure 3a). Cell numbers at 14 days and 21 days were the highest using fibrin gel seeding, the difference being significant compared with direct seeding at all time-points. Furthermore, cell numbers increased significantly with time in the case of fibrin seeding ($p < 0.05$), while no increase in cell numbers was observed with micromass and direct seeding. Based on the DNA quantification and methylene blue results direct seeding was excluded from further analysis.

Sulphated GAG and collagen assays were implemented in order to quantify the ECM production of hASCs seeded by fibrin gel or micromass techniques (Figure 3b,c). At 14 days, collagen production was significantly induced by fibrin seeding while the difference in sGAG production between the two seeding methods was not significant. The superiority of the fibrin seeding method was evident at 21 days as fibrin seeding significantly enhanced both the sulphated GAG and collagen production of hASCs compared with micromass seeding. Collagen production increased significantly with time in the case of fibrin seeding ($p < 0.05$), while the collagen content of micromass-seeded hASCs decreased significantly during the culture period ($p < 0.05$).

The sGAG–hydroxyproline ratio was used to determine whether the composition of the ECM produced by differentiated hASCs was similar to that of AF cells and native AF tissue (Mwale *et al.*, 2004). At both time-points, the sGAG/hydroxyproline ratio was similar for hASCs and AF cells, both seeded with fibrin (Figure 3d). Interestingly, the sGAG–hydroxyproline ratio increased significantly with time in the case of micromass-seeded hASCs. At day 21, the sGAG–hydroxyproline ratio for micromass-seeded hASCs was significantly higher than to that of fibrin gel-seeded hASCs and AF cells.

3.6. Histological evaluation of scaffolds seeded with hASCs

PicroSirius red staining of the collagen matrix produced in the scaffolds was in agreement with the quantification of total collagen content (Figures 3c and 4). Only fibrin-seeded hASCs showed abundant deposition of collagen inside the pore channels (Figure 4b). Importantly, polarized light showed the formation and alignment of collagen fibres in this condition (Figure 4f). In contrast, scaffolds seeded with hASCs using the micromass seeding method (Figure 4) and the AF cell control (Figure 4d) showed only weak collagen formation and no collagen fibres were detected using polarized light (Figure 4g,h).

3.7. Gene expression of differentiated hASCs and native AF cells in the scaffolds

All samples showed expression of aggrecan, decorin, collagen type I, type II and type V at 14 days and 21 days of

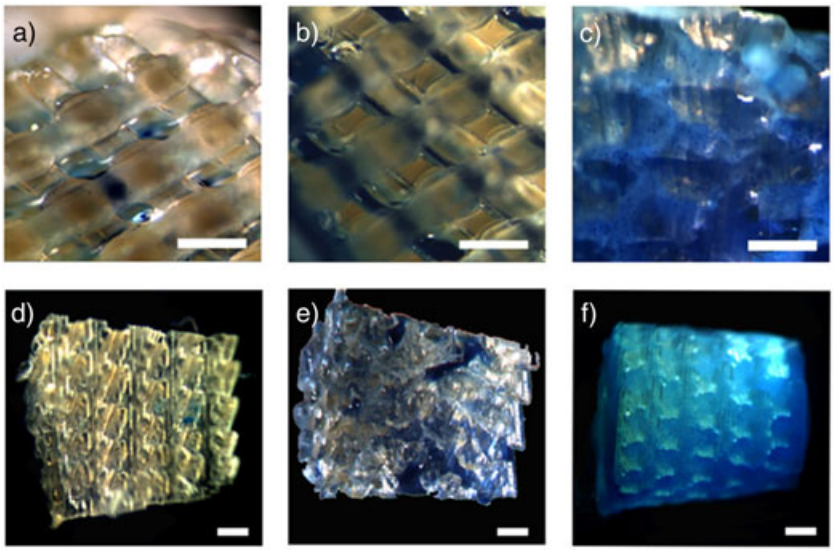

Figure 2. Methylene blue staining of differentiated human adipose-derived stem cells (hASC) seeded with direct (a,d), micromass (b,e) and fibrin gel (c,f) techniques in scaffolds at 1 day (a,b,c) and at 14 days (d,e,f). Bar: 500 μm.

DOI: 10.1002/term

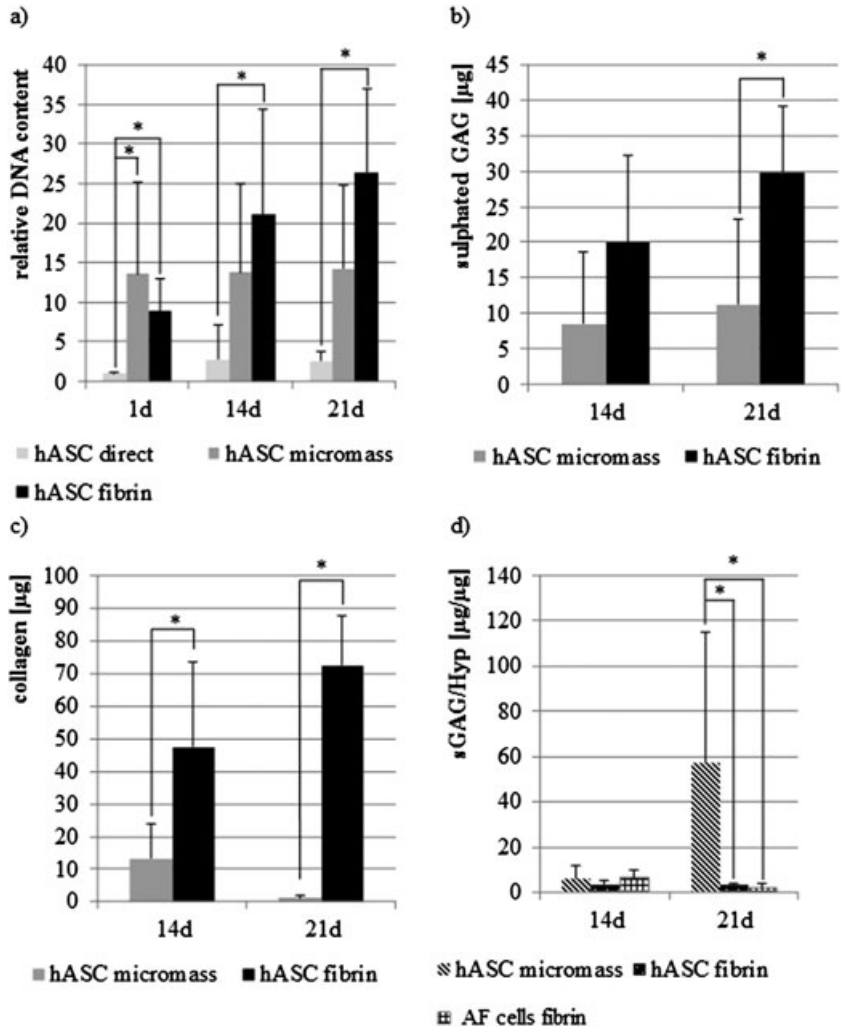

Figure 3. Relative DNA content of differentiated human adipose-derived stem cells (hASCs) seeded in the scaffolds by (a) direct, micromass and fibrin seeding, after 1, 14 and 21 days of culture. (b) Sulphated glycosaminoglycan (sGAG) content and (c) total collagen content of differentiated hASCs seeded by micromass and fibrin seeding at 14 days and at 21 days of culture. (d) Sulphated GAG/hydroxyproline ratio of differentiated hASCs seeded by micromass and fibrin seeding and fibrin-seeded human annulus fibrosus (AF) cells at 14 days and at 21 days of culture. The results are expressed as mean ± standard deviation (*$p < 0.05$).

culture in hASC and AF cell-seeded scaffolds (Figure 5). No statistical differences between the gene expression profiles of fibrin gel-seeded hASCs and native human AF cells were found. Decorin and collagen type II were expressed similarly in fibrin gel-seeded hASCs and AF cells. In contrast, aggrecan, collagen type I and type II

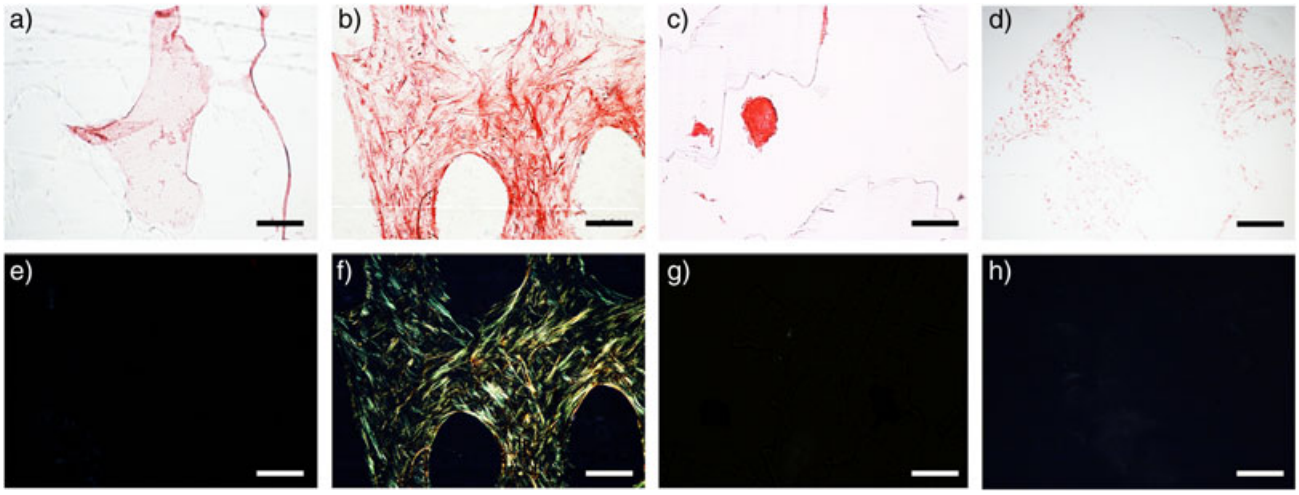

Figure 4. PicroSirius red staining of collagen visualized by normal (a–d) and polarized light (e–h), 21 days after seeding human adipose-derived stem cells (hASCs) in the scaffolds by fibrin gel (b,f) and micromass (c,g) seeding, and 21 days after seeding human annulus fibrosus cells by fibrin gel (d, h). A blank scaffold with only fibrin is shown in (a) and (e). Bar: 200 µm. 'Correction added on 14 November 2016, after first online publication: The legend for figure 4 has been amended to correctly identify the results.'

DOI: 10.1002/term

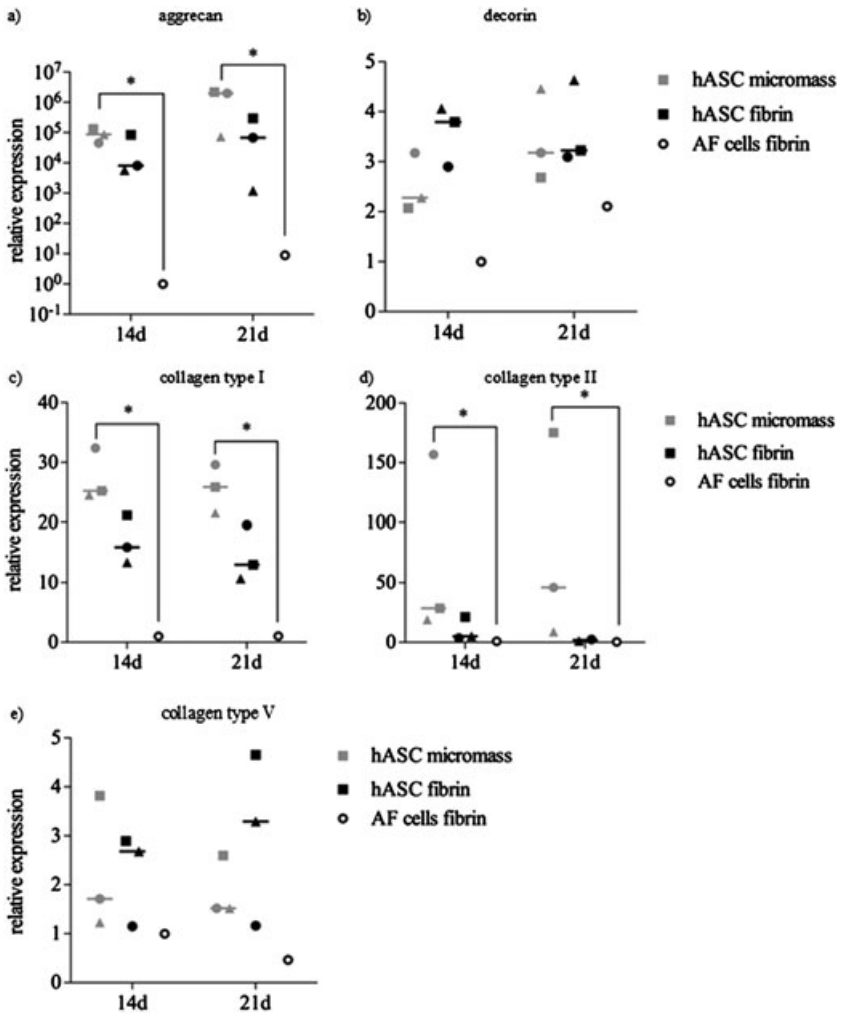

Figure 5. The relative expression of (a) aggrecan, (b) decorin, (c) collagen type I, (d) collagen type II and (e) collagen type V by differentiated human adipose-derived stem cells (hASCs) and human annulus fibrosus (AF) cells in the scaffolds at 14 days and at 21 days of culture. The results are presented relative to the mean expression in human AF cells at 14 days. The different symbols in the figure indicate different donors. Median expression is marked with a horizontal line (*$p < 0.05$).

gene expressions of micromass-seeded hASCs were significantly higher compared with the expressions of the AF cells at both time-points.

4. Discussion

At present, there are no effective treatment strategies to regenerate and repair ruptured AF tissue. Therefore, there is an unmet clinical need for an effective cell-based strategy to restore the biological and biomechanical functions of degenerated AF tissue. Harvested AF cells from the disc have been studied as a cell source for AF engineering (Gruber *et al.*, 2009). However, the use of AF cells has encountered major challenges because of the extremely limited availability of the cells in addition to senescence and decreased or altered ECM production (Gruber *et al.*, 2007). Transplantation of hASCs differentiated towards AF-like cells is therefore an attractive alternative. This is the first study describing an efficient approach to engineering AF tissue *in vitro* using fibrin gel seeding and differentiation of hASCs stimulated by TGF-β3 in AF-mimetic PTMC scaffolds.

Owing to the high biological and functional complexity of AF tissue structure, scaffolds for AF tissue engineering require precise and sophisticated geometries. The results of the present study show that the combination of fibrin-seeded hASCs and the scaffold architecture play a significant role in appropriate AF-like matrix production and collagen alignment. This is in agreement with a previous study showing that collagen orientation is controlled by large-scale microstructures in a scaffold for vascular tissue engineering (Engelmayr *et al.*, 2006). Similarly, (de Mulder *et al.*, 2013) used thermal-induced phase separation to prepare a scaffold for meniscus repair, in which collagen fibres were oriented through the channel-like pore architecture of the scaffold. However, this technique does not allow sufficient control of the pore architecture, which is essential to reach the optimal reproduction of the AF tissue structure and function. In consequence, a 3D scaffold with specific micro-architecture able to mimic with high precision the complex architecture of native AF will guide the cells and the produced collagen to follow the porous orientation and therefore reproduce the desired structure and function.

Annulus fibrosus tissue is composed of 15–25 loosely connected concentric lamellae consisting of highly

DOI: 10.1002/term

organized collagen fibres (Marchand and Ahmed, 1990). In the lamella, collagen fibres run parallel and are oriented at an angle-ply of 30°, from the transverse section of the IVD, at the outer side of the AF evolving to 45° at the inner side (Cassidy *et al.*, 1989). Each lamella is alternated with another lamella in the opposite direction. Only a few studies have reported on the development of a scaffold reproducing the complex architecture of the collagen fibres in the AF. Nerurkar *et al*. (2009) reported for the first time an electrospun membrane that replicates the specific angle-ply displayed by the collagen fibres. However, owing to limitations of the electrospinning approach, the membrane scaffold was built with only two layers, and cannot be considered as full-sized three-dimensional scaffold. The use of a lamellar silk scaffold has also been reported. However, these approaches cannot be adapted to our purpose, either because of the isotropic random pore structure obtained by the scaffold preparation process used, which will influence the biomechanical performance (Park *et al.*, 2012), or because it does not allow the fabrication of a full-sized three-dimensional scaffold that is required to repair a herniated disc (Bhattacharjee *et al.*, 2012).

Therefore, none of these previous strategies reported in the literature describe a scaffold design that allows precise control of the complex organization and orientation of the collagen bundles from native tissue. This limitation may be the major reason explaining the inability to precisely reproduce oriented collagen fibres in previous work. In consequence, the work presented here is the first study describing a 3D scaffold designed with an oriented channel-like pore architecture that reproduces the complex structure of AF tissue. The scaffold design was achieved by precisely respecting the complex and typical multilamellar organization and angle-ply of the native AF collagen (see Figure 1a,b) and built with a high precision by stereolithography. Furthermore, the truncated cone geometry of the scaffold was designed in order to prevent the risk of scaffold extrusion after implantation in the disc defect. This specific geometry allows the use of the scaffold as a plug and increases the stability of the implanted scaffold inside the defect.

To obtain efficient *in vitro* AF differentiation, not only a suitable scaffold design is required but also the differentiation medium for hASCs needs to be defined. Therefore, in the first part of this study a suitable AF differentiation medium for hASCs in two-dimensional (2D) culture was defined. The importance of TGF-β1 or TGF-β3 to maintain the AF cell phenotype *in vitro* has been reported in several studies (Colombini *et al.*, 2014; Guillaume *et al.*, 2014). However, the present study appears to be the first to compare the effects of TGF-β1 and TGF-β3 or their combination on hASC proliferation and differentiation towards AF tissue. Importantly, all the differentiation experiments in then present study were done under serum-free conditions to allow direct application of the results to clinical therapy. According to the biochemical and histological analysis of the micromass cultures, sGAG and proteoglycan production were substantially enhanced in the presence of TGF-β3 (see the Supplementary material online, Figure S1). In addition, the gene expression of aggrecan, which is the most abundant proteoglycan in AF tissue (Roughley *et al.*, 2006), was upregulated in hASCs cultured in the presence of TGF-β3, further confirming the role of TGF-β3 in promoting hASC differentiation towards AF-like cells. The results are in line with a recent study where TGF-β3 supplementation stimulated matrix deposition of AF cells *in vitro* (Guillaume *et al.*, 2014). Furthermore, TGF-β3 has been shown to upregulate aggrecan, collagen type I and II gene expression in an *in vitro* full-organ disc/endplate culture system (Haschtmann *et al.*, 2012). Although TGF-β1 has been previously demonstrated to promote cellular proliferation and collagen production of various human cells, including AF cells (Jenner *et al.*, 2007; Wipff and Hinz, 2008; Turner *et al.*, 2014), TGF-β1 showed a negligible effect on AF differentiation of hASCs when supplemented alone. Hegewald *et al.* (2014) consistently showed no significant benefit of addition of TGF-β1 in 3D culture of AF cells. In the present study, the aggrecan expression was the highest when TGF-β1 was used in combination with TGF-β3, however, the difference was not significant. Furthermore, no significant differences were found in the expression of decorin and collagen types I and II between the different medium groups. As the addition of TGF-β1 to the TGF-β3-supplemented medium did not give any significant benefit, DM3 was considered the most suitable AF differentiation medium for hASCs.

In addition to the composition of the differentiation medium, different cell seeding strategies have been shown to have a major effect on stem cell fate (Ameer *et al.*, 2002; Colombini *et al.*, 2014). However, an efficient cell seeding strategy that supports mesenchymal stem cell differentiation towards AF tissue has not been reported previously. We therefore wanted to find an efficient cell seeding strategy to stimulate hASC differentiation towards the AF phenotype. Direct seeding was used as a reference method because this approach is traditionally used to seed cells into 3D scaffolds (Haimi *et al.*, 2009b), and it has been shown to be suitable for AF cell culture in 3D scaffolds prepared by stereolithography (Blanquer *et al.*, 2013). Interestingly, the results of the present study showed that hASCs seeded by direct seeding were only poorly attached and spread throughout the scaffolds when compared with micromass and fibrin gel seeding. Moreover, the cell seeding efficiency was extremely low in the case of direct seeding. These results are consistent with a previous study demonstrating major challenges in obtaining a uniform cell distribution in 3D scaffolds using direct cell seeding (Lee *et al.*, 2005). Micromass seeding was chosen because it has been used as a standard technique to enhance AF differentiation of ASCs in 3D scaffolds (Tapp *et al.*, 2008; Gruber *et al.*, 2010). Nevertheless, in the *in vitro* studies of Gruber *et al.* (2010) the micromass seeding of hASCs even in the presence of TGF-β3 did not allow a sufficient AF-like matrix production especially in terms of sufficient collagen production. Scaffolds seeded with hydrogels such as hyaluronic acid

DOI: 10.1002/term

(Nesti *et al.*, 2008) and fibrin (Sha'ban *et al.*, 2008) in combination with cells have been suggested to be useful in AF tissue engineering. In order to trigger hASC differentiation towards AF cells, fibrin gel seeding was tested because recent studies have demonstrated the importance of fibrin in maintaining the typical phenotype of AF cells (Colombini *et al.*, 2014) and promoting the production of ECM (Sha'ban *et al.*, 2008).

Fibrin seeding of hASCs resulted in significantly enhanced proliferation and AF-like ECM formation compared with the other seeding strategies. The higher sGAG content of the fibrin-seeded scaffolds may be explained by a higher retention of synthesized glycosaminoglycans in the fibrin gel compared with micromass seeding (Ameer *et al.*, 2002). Moreover, fibrin seeding resulted in an abundant production of collagen, which is the main ECM component of AF tissue (Roughley, 2004). Collagen production increased significantly from 14 days to 21 days, indicating that the fibrin seeding method together with the designed scaffold fully support the production of collagenous AF-like matrix by the hASCs. Not only the production of sGAG and collagen was significantly upregulated, but the collagen was also organized in a specific manner. PicroSirius red staining of collagen showed that the AF-mimetic architecture of the scaffold led to regularly packed and aligned collagen bundles inside the designed pore channels, which is essential for the biomechanical function of AF tissue (Nerurkar *et al.*, 2010). This result is remarkable as, in the present study, abundant collagen production and bundle formation in a 3D porous structure was obtained under static conditions without mechanical stimulation. Although the pore characteristics of the scaffold obtained have not yet been optimized, the results obtained in the present study do show that collagen bundles can be created and that several collagen bundles appear to be aligned along the pore. This represents considerable progress in this field.

The sGAG to hydroxyproline ratio can be used as a specific parameter to distinguish AF from nucleus pulposus tissue. It was found that this ratio was similar for AF cells (approximately 2:1) and differentiated hASCs (approximately 3:1), both seeded with fibrin and cultured for 21 days. These ratios correspond closely to the value reported for native human AF tissue (approximately 2:1) (Mwale *et al.*, 2004). In contrast, the sGAG to hydroxyproline ratio for micromass-seeded hASCs was around 57:1, which is significantly different from the ratios for fibrin gel-seeded hASCs and AF cells, tending towards the ratio reported for nucleus pulposus tissue (26:1) (Mwale *et al.*, 2004).

To further verify the AF phenotype obtained, AF-specific markers were quantified on the mRNA level. Aggrecan and decorin are the most overexpressed proteoglycans while collagen type I and II are the major collagens present in the ECM of AF tissue (Roughley *et al.*, 2006). However, these collagens are not specific for AF tissue alone. Instead, collagen type V has been shown to be a more specific marker for AF tissue, distinguishing AF cells from nucleus pulposus cells and chondrocytes (Clouet *et al.*, 2009). In the present study, micromass and fibrin-seeded hASCs, as well as fibrin-seeded AF cells, expressed similar levels of collagen type V. As a result of the notable donor variation of the mRNA expression, results were shown as a scatter plot instead of a box plot to demonstrate the response of individual donors (Figure 5). This donor variation is a typical of hASCs and other adult stem cells, as has been described previously (Chou *et al.*, 2011; Bieback *et al.*, 2012; Kyllonen *et al.*, 2013). Nevertheless, our results show that the AF-related gene expression profiles of fibrin-seeded hASCs and human AF cells were not significantly different. These results, together with the sGAG to hydroxyproline ratio of 3:1, indicate the potential of fibrin seeding of hASCs in AF tissue engineering. In contrast, micromass-seeded hASCs differed significantly from the AF cells in terms of aggrecan, collagen type I and collagen type II gene expression.

5. Conclusions

The present study demonstrated that stimulation with TGF-β3 induces efficient differentiation of hASCs towards AF-like cells. Furthermore, ECM production by hASCs seeded in an AF-mimetic PTMC scaffold was evaluated using direct, fibrin gel or micromass seeding in a defined differentiation medium supplemented with TGF-β3. The scaffold designed was prepared by stereolithography in order to mimic the complex architecture of native AF tissue in terms of collagen fibre organization and orientation. Fibrin gel seeding allowed more uniform cell attachment and spreading in the scaffold compared with the other seeding methods. Importantly, fibrin seeding significantly stimulated sGAG and collagen production with a ratio of sGAG to collagen that was similar to that of native AF tissue. Moreover, it could be observed that several collagen fibres were arranged in regularly aligned bundles in the designed pore channels. Only when the fibrin seeding method was used was the phenotype of the differentiated hASCs similar to that of native AF cells. In conclusion, fibrin gel seeding of hASCs in an AF-mimetic PTMC scaffold and subsequent culturing in the presence of TGF-β3 is a strategy with great potential to engineer AF tissue *in vitro*.

Acknowledgement

This work was funded by the AO foundation and Academy of Finland. In addition, we would like to acknowledge Dr Zhen Li, Dr Sibylle Grad, Dr David Eglin and Prof. Dr Mauro Alini of the AO Research Institute for contributions to this work.

Conflict of interest

The authors have declared that there is no conflict of interest.

DOI: 10.1002/term

References

Ameer GA, Mahmood TA, Langer R, 2002; A biodegradable composite scaffold for cell transplantation. *J Orthop Res* **20**: 16–19.

Bao QB, Mccullen GM, Higham PA, *et al*. 1996; The artificial disc: Theory, design and materials. *Biomaterials* **17**: 1157–1167.

Bhattacharjee M, Miot S, Gorecka A, *et al*. 2012; Oriented lamellar silk fibrous scaffolds to drive cartilage matrix orientation: Towards annulus fibrosus tissue engineering. *Acta Biomater* **8**: 3313–3325.

Bibby SR, Jones DA, Lee RB, *et al*. 2001; The pathophysiology of the intervertebral disc. *Joint Bone Spine* **68**: 537–542.

Bieback K, Hecker A, Schlechter T, *et al*. 2012; Replicative aging and differentiation potential of human adipose tissue-derived mesenchymal stromal cells expanded in pooled human or fetal bovine serum. *Cytotherapy* **14**: 570–583.

Blanquer SBG, Haimi SP, Poot AA, *et al*. 2013; Effect of pore characteristics on mechanical properties and annulus fibrosus cell seeding and proliferation in designed ptmc tissue engineering scaffolds. *Macromol Symp* **334**: 75–81.

Blanquer SBG, Grijpma DW, Poot AA, 2015; Delivery systems for the treatment of degenerated intervertebral discs. *Adv Drug Deliv Rev* **84**; 172–187.

Bron JL, Helder MN, Meisel HJ, *et al*. 2009; Repair, regenerative and supportive therapies of the annulus fibrosus: achievements and challenges. *Eur Spine J* **18**: 301–313.

Cassidy JJ, Hiltner A, Baer E, 1989; Hierarchical structure of the intervertebral-disk. *Connect Tissue Res* **23**: 75–88.

Chou YF, Zuk PA, Chang TL, *et al*. 2011; Adipose-derived stem cells and bmp**2**: Part 1. Bmp2-treated adipose-derived stem cells do not improve repair of segmental femoral defects. *Connect Tissue Res* **52**: 109–118.

Clouet J, Grimandi G, Pot-Vaucel M, *et al*. 2009; Identification of phenotypic discriminating markers for intervertebral disc cells and articular chondrocytes. *Rheumatology* **48**: 1447–1450.

Colombini A, Lopa S, Ceriani C, *et al*. 2014; *In vitro* characterization and *in vivo* behavior of human nucleus pulposus and annulus fibrosus cells in clinical-grade fibrin and collagen-enriched fibrin gels. *Tissue Eng Part A* **21**(3-4): 793–802.

Coppes MH, Marani E, Thomeer RTWM, *et al*. 1990; Innervation of annulus fibrosis in low-back-pain. *Lancet* **336**: 189–190.

De Mulder ELW, Hannink G, Verdonschot N, *et al*. 2013; Effect of polyurethane scaffold architecture on ingrowth speed and collagen orientation in a subcutaneous rat pocket model. *Biomed Mater* **8**: 025004.

Disch AC, Schmoelz W, Matziolis G, *et al*. 2008; Higher risk of adjacent segment degeneration after floating fusions: long-term outcome after low lumbar spine fusions. *J Spinal Disord Tech* **21**: 79–85.

Dominici M, Le Blanc K, Mueller I, *et al*. 2006; Minimal criteria for defining multipotent mesenchymal stromal cells. The International Society for Cellular Therapy position statement. *Cytotherapy* **8**: 315–317.

Ebara S, Iatridis JC, Setton LA, *et al*. 1996; Tensile properties of nondegenerate human lumbar anulus fibrosus. *Spine* **21**: 452–461.

Edwards CA, Obrien WD, 1980; Modified assay for determination of hydroxyproline in a tissue hydrolyzate. *Clin Chim Acta* **104**: 161–167.

Engelmayr GC, Papworth GD, Watkins SC, Mayer JE, Sacks MS, 2006; Guidance of engineered tissue collagen orientation by large-scale scaffold microstructures. *J Biomech* **39**: 1819–1831.

Fazzalari NL, Costi JJ, Hearn TC, *et al*. 2001; Mechanical and pathologic consequences of induced concentric anular tears in an ovine model. *Spine* **26**: 2575–2581.

Fink T, Lund P, Pilgaard L, *et al*. 2008; Instability of standard pcr reference genes in adipose-derived stem cells during propagation, differentiation and hypoxic exposure. *BMC Mol Biol* **9**.

Gabrielsson BG, Olofsson LE, Sjogren A, *et al*. 2005; Evaluation of reference genes for studies of gene expression in human adipose tissue. *Obes Res* **13**: 649–652.

Gruber HE, Ingram JA, Norton HJ, *et al*. 2007; Senescence in cells of the aging and degenerating intervertebral disc – immunolocalization of senescence-associated beta-galactosidase in human and sand rat discs. *Spine* **32**: 321–327.

Gruber HE, Hoelscher G, Ingram JA, *et al*. 2009; Culture of human anulus fibrosus cells on polyamide nanofibers extracellular matrix production. *Spine* **34**: 4–9.

Gruber HE, Deepe R, Hoelscher GL, *et al*. 2010; Human adipose-derived mesenchymal stem cells: direction to a phenotype sharing similarities with the disc, gene expression profiling, and coculture with human annulus cells. *Tissue Eng* **16**: 2843–2860.

Guillaume O, Daly A, Lennon K, *et al*. 2014; Shape-memory porous alginate scaffolds for regeneration of the annulus fibrosus: effect of TGF-beta 3 supplementation and oxygen culture conditions. *Acta Biomater* **10**: 1985–1995.

Guterl CC, See EY, Blanquer SBG, *et al*. 2013; Challenges and strategies in the repair of ruptured annulus fibrosus. *Eur Cell Mater* **25**: 1–21.

Haimi S, Moimas L, Pirhonen E, *et al*. 2009a; Calcium phosphate surface treatment of bioactive glass causes a delay in early osteogenic differentiation of adipose stem cells. *J Biomed Mater Res A* **91**: 540–547.

Haimi S, Suuriniemi N, Haaparanta AM, *et al*. 2009b; Growth and osteogenic differentiation of adipose stem cells on pla/bioactive glass and pla/beta-tcp scaffolds. *Tissue Eng Part A* **15**: 1473–1480.

Haschtmann D, Ferguson SJ, Stoyanov JV, 2012; Bmp-2 and tgf-beta3 do not prevent spontaneous degeneration in rabbit disc explants but induce ossification of the annulus fibrosus. *Eur Spine J* **21**: 1724–1733.

Hegewald AA, Cluzel J, Kruger JP, *et al*. 2014; Effects of initial boost with TGF-beta 1 and grade of intervertebral disc degeneration on 3D culture of human annulus fibrosus cells. *J Orthop Surg Res* **9**: 73.

Jenner JM, Van Eijk F, Saris DB, Willems WJ, Dhert WJ, Creemers LB, 2007; Effect of transforming growth factor-beta and growth differentiation factor-5 on proliferation and matrix production by human bone marrow stromal cells cultured on braided poly lactic-co-glycolic acid scaffolds for ligament tissue engineering. *Tissue Eng* **13**: 1573–1582.

Kuh SU, Zhu YR, Li J, *et al*. 2009; A comparison of three cell types as potential candidates for intervertebral disc therapy: annulus fibrosus cells, chondrocytes, and bone marrow derived cells. *Joint Bone Spine* **76**: 70–74.

Kyllonen L, Haimi S, Mannerstrom B, *et al*. 2013; Effects of different serum conditions on osteogenic differentiation of human adipose stem cells *in vitro*. *Stem Cell Res Ther* **4**: 17

Lee CR, Grad S, Gorna K, *et al*. 2005; Fibrin–polyurethane composites for articular cartilage tissue engineering: a preliminary analysis. *Tissue Eng* **11**: 1562–1573.

Lindroos B, Suuronen R, Miettinen S, 2011; The potential of adipose stem cells in regenerative medicine. *Stem Cell Rev Rep* **7**: 269–291.

Marchand F, Ahmed AM, 1990; Investigation of the laminate structure of lumbar disc anulus fibrosus. *Spine* **15**: 402–410.

Melchels FPW, Feijen J, Grijpma DW, 2010; A review on stereolithography and its applications in biomedical engineering. *Biomaterials* **31**: 6121–6130.

Mwale F, Roughley P, Antoniou J, 2004; Distinction between the extracellular matrix of the nucleus pulposus and hyaline cartilage: a requisite for tissue engineering of intervertebral disc. *Eur Cell Mater* **8**: 58–64.

Nerurkar NL, Baker BM, Sen S, *et al*. 2009; Nanofibrous biologic laminates replicate the form and function of the annulus fibrosus. *Nat Mater* **8**: 986–992.

Nerurkar NL, Elliott DM, Mauck RL, 2010; Mechanical design criteria for intervertebral disc tissue engineering. *J Biomech* **43**: 1017–1030.

Nesti LJ, Li WJ, Shanti RM, *et al*. 2008; Intervertebral disc tissue engineering using a novel hyaluronic acid-nanofibrous scaffold (HANFS) amalgam. *Tissue Eng Part A* **14**: 1527–1537.

Orozco L, Soler R, Morera C, *et al*. 2011; Intervertebral disc repair by autologous mesenchymal bone marrow cells: a pilot study. *Transplantation* **92**: 822–828.

Park SH, Gil ES, Mandal BB, *et al*. 2012. Annulus fibrosus tissue engineering using lamellar silk scaffolds. *J Tissue Eng Regen Med* **6**(Suppl 3): s24–s33.

Pfaffl MW, 2001; A new mathematical model for relative quantification in real-time *RT-PCR Nucl Acids Res* **29**: e45.

Richardson SM, Hoyland JA, Mobasheri R, *et al*. 2010; Mesenchymal stem cells in regenerative medicine: opportunities and challenges for articular cartilage and intervertebral disc tissue engineering. *J Cell Physiol* **222**: 23–32.

Roughley P, Martens D, Rantakokko J, *et al*. 2006; The involvement of aggrecan polymorphism in degeneration of human intervertebral disc and articular cartilage. *Eur Cell Mater* **11**: 1–7.

Roughley PJ, 2004; Biology of intervertebral disc aging and degeneration – involvement of the extracellular matrix. *Spine* **29**: 2691–2699.

Schuller-Ravoo S, Teixeira SM, Feijen J, *et al*. 2013; Flexible and elastic scaffolds for cartilage tissue engineering prepared by stereolithography using poly(trimethylene carbonate)-based resins. *Macromol Biosci* **13**: 1711–1719.

Sha'ban M, Yoon SJ, Ko YK, *et al*. 2008; Fibrin promotes proliferation and matrix production of intervertebral disc cells cultured in three-dimensional poly(lactic-co-glycolic acid) scaffold. *J Biomater Sci Polym Ed* **19**: 1219–1237.

Skoog SA, Goering PL, Narayan RJ, 2014. Stereolithography in tissue engineering. *J Mater Sci Mater Med* **25**: 845–856.

Tapp H, Deepe R, Ingram JA, *et al*. 2008; Adipose-derived mesenchymal stem cells from the sand rat: transforming growth factor beta and 3D co-culture with human disc cells stimulate proteoglycan and collagen type I rich extracellular matrix. *Arthritis Res Ther* **10**: R89.

Turner KG, Ahmed N, Santerre JP, *et al*. 2014; Modulation of annulus fibrosus cell alignment and function on oriented nanofibrous polyurethane scaffolds under tension. *Spine J* **14**: 424–434.

Vyner MC, Li AN, Amsden BG, 2014; The effect of poly (trimethylene carbonate) molecular weight on macrophage behavior and enzyme adsorption and conformation. *Biomaterials* **35**: 9041–9048.

Wipff PJ, Hinz B, 2008. Integrins and the activation of latent transforming growth factor beta1 – an intimate relationship. *Eur J Cell Biol* **87**: 601–615.

Zhang Z, Kuijer R, Bulstra SK, *et al*. 2006; The *in vivo* and *in vitro* degradation behavior of poly(trimethylene carbonate). *Biomaterials* **27**: 1741–1748.

Supporting information on the internet

Additional supporting information may be found in the online version of this article at the publisher's web-site.

Figure S1. (a) DNA content; (b) sulphated GAG content; (c) toluidine blue staining; (d) aggrecan gene expression of hASC micromasses cultured for 21 days in chondrogenic medium

Figure S2. Methylene blue-stained scaffold with fibrin and without hASCs, demonstrating that fibrin gel alone did not take up significantly the methylene blue dye